A Simulation Study on Dynamics of Dendrimer−Polymer Conjugates

Tong Zhou and Shing Bor Chen*

Department of Chemical and Biomolecular Engineering, National University of Singapore, Singapore 117576, Republic of Singapore

Received May 17, 2006; Revised Manuscript Received June 29, 2006

ABSTRACT: Brownian dynamics simulation is conducted to investigate the dynamics of dendrimer−polymer conjugates on the basis of a coarse-grained bead−spring model. The grafted polymers are found to slow the global dynamics of the dendrimer core. Because of the structural difference between the two moieties, the translational and rotational diffusivities of a conjugate show different scaling behaviors from those for a dendrimer, but in principle follow a Stokes−Einstein fashion, analogous to polymers of other types. When the grafted chains are long enough, they become brushlike, evidenced by the scaling behavior of the end-to-end distance as well as the chain-length dependence of the rotational relaxation time. For the range of chain length investigated, it is found that the brushlike grafted polymers still fall within the dilute regime. Thereby the interchain interactions are not strong enough to render a change in the scaling behavior of rotation relaxation in comparison with an isolated rodlike polymer.

1. Introduction

A dendrimer is a branched polymer with a well-defined treelike structure and can serve as a potential effective device for gene delivery, boron neutron capture therapy, molecular recognition, and drug delivery.[1,2] To satisfy biological demands in practical applications, some dendrimers are modified with biologically friendly molecules. For instance, poly(ethylene glycol) (PEG) was grafted to a poly(aryl ether) dendrimer and an amino-terminated polyamidoamine (PAMAM) dendrimer to form a water-soluble dendrimer−polymer conjugate.[3,4] Apart from better satisfaction for biological demands, dendrimer−polymer conjugates are found to have a higher encapsulation ability than that of the dendrimer counterpart.[4,5] This paper focuses on the conjugate dynamics to complement our prior investigation on its structural behavior.[5]

The structural properties of dendrimers have been extensively investigated during last two decades. The dendrimer size is predicted to scale as $N^{1/5}P^{2/5}(G+1)^{2/5}$, $N^{1/4}P^{1/4}(G+1)^{1/4}$, and $N^{1/3}$ in a good, Θ, and poor solvent, respectively,[6,7] where N is the number of monomers, P is the spacer length, and G is the generations of the dendrimer. The outer segments of a dendrimer can fold back and stay in the interior space,[8−12] contrary to the first thought that the dendrimer has a loose core and a dense shell. For a dendrimer−polymer conjugate, we have found that the back-folding of terminal groups is reduced because the grafted linear polymers give rise to an increased steric effect.[5] Therefore, the dendrimer has more interior space to encapsulate guest molecules. Moreover, the grafted chains indeed become brushlike when they are long enough.

For dendrimer dynamics, there have existed several experimental, theoretical, and simulation studies. Meltzer et al. applied NMR to determine spin−lattice relaxation times and spin−spin relaxation times of PAMAM.[13,14] Mourey et al.[15] employed size exclusion chromatography to measure the intrinsic viscosity and the hydrodynamic radius of polyether, the latter of which was found to approximately grow linearly with G. A similar finding was also reported for poly(propyleneimine) dendrimers from experiments.[16,17] Besides the experimental studies, theoretical modeling on dendrimer dynamics has been carried out. Mansfield and Klushin[18] calculated the upper and lower bounds of hydrodynamic radius R_h of PAMAM based on preaveraged hydrodynamic interaction (HI). At small G, the upper and lower bounds of R_h are close to each other and in good agreement with the radius of gyration R_g. However, neither the upper bound nor the lower bound of R_h grows linearly with G. This behavior was reproduced by other researchers using a similar approach.[19−21] Alternatively, Mansfield used a novel capacitance-analogy method to compute R_h and obtained a reasonable trend with varying G.[11] Rouse dynamics of a dendrimer in the Θ condition was examined by Cai and Chen,[22] who later took into account the preaveraged HI and excluded volume effect in a following work.[23] Various relaxation times were determined, apart from diffusivity. Their theory predicted an equal relaxation time for the dendrimer rotation and size fluctuation. The rotational relaxation time, however, showed a stronger G dependence than the experimental data.

As for computer simulations of dendrimer dynamics, a molecular dynamics simulation was employed by Murat and Grest[10] and Karatasos et al.[24] Treating the solvent as a continuum, Murat and Grest examined the relaxation times of internal fluctuation of dendrimer size. Because the dependence of the simulated relaxation times on the generation number was very noisy, no quantitative conclusion could be drawn. Karatasos et al. considered explicit solvent molecules to investigate the translational diffusion, global rotational motions, and local segment dynamics of AB_2 dendrimers in the Θ condition. The long-time diffusivity of dendrimers appeared to be inversely proportional to the square root of the molecular weight. The global rotation slows down for a higher number of generations, but becomes indistinguishable for G3 and G4 dendrimers. The autocorrelation functions of bond vectors decay faster for a lower number of generations. Outer bond vectors relax faster than interior ones. Applying Brownian dynamics simulation, Lyulin et al.[25] systematically explored the dynamics of neutral and charged dendrimers with consideration of fluctuating HI, excluded volume effect, and electrostatic interaction via the Debye−Huckle approximation. Both global and local dynamics were studied and compared with the theoretical prediction[22,23] and the experimental data.[17]

* Corresponding author. E-mail: checsb@nus.edu.sg.

10.1021/ma061103q CCC: $33.50
Published on Web 08/18/2006

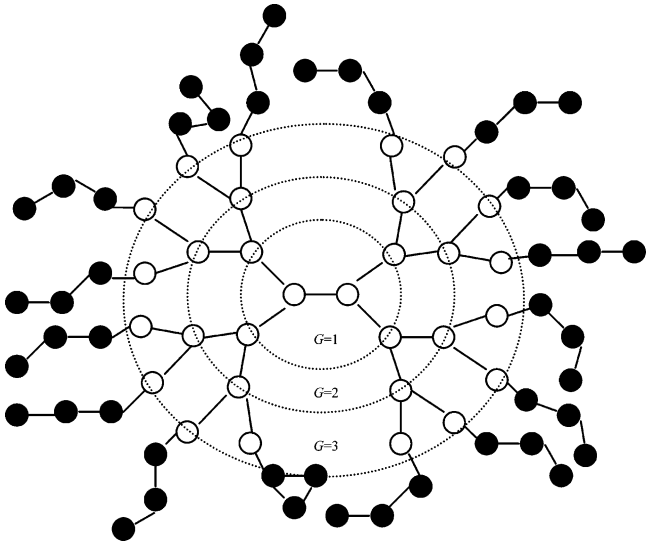

Figure 1. Schematic of a dendrimer−polymer conjugate. Open circles represent the beads of the dendrimer core, while the filled circles are the beads of the grafted polymers.

For the dynamics of conjugates in a melt state, Stark et al.[26] used X-ray scattering and quasielastic neutron scattering to study carbosilane dendrimers up to three generations with perfluorohexyl groups on the surface. The dynamic structure factor of the labeled dendrimer core was analyzed to deduce the segmental translational diffusivity of the dendrimer core and the rotational diffusivity of the surface groups. They reported that the segmental diffusivity of G3 with surface groups was reduced by a factor of 7.4 compared to that of G3 only, while an increasing generation number slightly decreased the rotational diffusivity of the surface groups. To our best knowledge, there exists no study on the dynamics of conjugates in a solvent.

We had applied Monte Carlo simulation to investigate the effect of grafted polymers on the structural properties of dendrimers in the previous work.[5] In view of the practical applicability and advantage of dendrimer−polymer conjugates in drug encapsulation, it is important to understand their dynamics as well. The present study employs Brownian dynamics simulation to examine the translational and rotational diffusivity of conjugates in a dilute solution and the influence of the attachment on various relaxation times. Because the dynamical properties simulated by Lyulin et al.[25] are of interest and relevance to our system, we follow some of their definitions and make comparison in this study.

2. Model and Simulation

We consider a dendrimer−polymer conjugate for which linear polymer chains (filled circles) are attached to a dendrimer (open circles), as shown in Figure 1. The architecture adopted here is a dendron emanating from two central connected trifunctional units (zeroth generation),[4,7,19] which is identical with that used in our previous paper.[5] The bonded spherical beads of the same mass are utilized to represent the monomers of the dendrimer and of the linear polymers by assuming the spacer length to be unity. The bonding energy is modeled by the energy of a harmonic spring:

$$U^{S} = k(r - l_0)^2 \tag{1}$$

with k being the spring constant, l_0 the equilibrium bond length, and r the distance between two bonded beads. In this study, the spring constant k is set to be 200 k_BT/l_0^2 to render the bond length fluctuation within 5% of l_0, where k_B is the Boltzmann constant and T is the absolute temperature. The interaction between nonbonded beads is described by a Lennard-Jones (LJ) potential:

$$U^{LJ} = 4w\left[\left(\frac{\sigma}{r}\right)^{12} - \left(\frac{\sigma}{r}\right)^{6}\right] \tag{2}$$

Using eq 2, the solvent quality is determined by the values of w and cutoff r_{cut}. We specify $\sigma = 0.8l_0$, $w = 0.3\ k_BT$, and $r_{cut} = 2.5\sigma$, as in the study of Rey et al.[27] Using these parameters, our test on free linear polymers finds that the squared end-to-end distance follows a power law with an exponent of 1.029,[5] thereby corresponding to a state near the Θ condition for linear polymers.

The total number of beads N in the dendrimer relates to its terminal generation G by the following equation:

$$N = 2^{G+2} - 2 \tag{3}$$

and the number of end beads N_{end} is

$$N_{end} = 2^{G+1} \tag{4}$$

We assume that each of the end beads is attached by a linear chain of N_{chain} bonded beads. Therefore, the total number of beads in the dendrimer−polymer conjugate is

$$N_{total} = N + N_{end}N_{chain} \tag{5}$$

For dendrimers without attached chains, we investigate the cases of G ranging from 2 to 5, corresponding to N from 14 to 126. For dendrimer−polymer conjugates, we fix $G = 3$ and vary the length of the attached chains from N_{chain}= 2 to 15, which corresponds to N_{total} between 62 and 270.

The motions of the beads are governed by the stochastic differential equations (SDE)[28] with negligence of the inertial term. In the $3N_{total}$ spatial coordinates, SDE in the absence of external flow can be expressed as

$$\mathbf{R}(t + \Delta t) = \mathbf{R}(t) + (\mathbf{M}\cdot\mathbf{F} + k_BT\nabla\cdot\mathbf{M})\Delta t + \sqrt{2}\mathbf{B}\cdot\Delta\mathbf{W} \tag{6}$$

with

$$\mathbf{M} = \mathbf{B}\cdot\mathbf{B}^{T} \tag{7}$$

In eq 6, $\mathbf{R}$ is a $3N_{total}$ vector representing the spatial coordinates of all the particles, $\mathbf{M}$ is the mobility tensor ($3N_{total} \times 3N_{total}$) depending on HI between all the particles, $\mathbf{F}$ is the $3N_{total}$ force vector determined by the gradient of the interaction potential

$$\mathbf{F} = -\nabla(U^{S} + U^{LJ}) \tag{8}$$

and $\Delta\mathbf{W}$ is a $3N_{total}$ vector arising from the Brownian motions of the particles, which is obtained by the Wiener process, and each component has zero mean and variance equal to Δt.

The most computation-intensive part at each time step in our simulation is the determination of the mobility tensor $\mathbf{M}$ and its decomposition to obtain $\mathbf{B}$ (see eq 7). We adopt the Ronte−Prager−Yamakawa tensor[29,30]

$$\mathbf{M}_{ij} = \begin{bmatrix} \frac{1}{6\pi\mu a}\mathbf{I} & (i=j) \\ \frac{1}{8\pi\mu r}\left[\left(1+\frac{2a^2}{3r^2}\right)\mathbf{I} + \left(1-\frac{2a^2}{r^2}\right)\frac{\mathbf{rr}}{r^2}\right] & (i\neq j,\ r\geq\sigma) \\ \frac{1}{6\pi\mu a}\left[\left(1-\frac{9r}{32a}\right)\mathbf{I} + \frac{3r}{32a}\frac{\mathbf{rr}}{r^2}\right] & (i\neq j,\ r<\sigma) \end{bmatrix} \tag{9}$$

for each pair of particles, where **I** is the unit tensor, μ is the solvent viscosity, and $a = \sigma/2$. Because the solvent is incompressible, $\nabla\cdot\mathbf{M}$ vanishes. The determination of **B** is usually done by the Cholesky decomposition.[31] To reduce the computation time, we use the Chebyshev polynomial approximation[32] to directly compute $\mathbf{B}\cdot\Delta\mathbf{W}$ instead. This method was first proposed by Fixman[33] and later improved by Jendrejack et al.[34] For detailed discussion, we refer the readers to the original work.

Hereafter, we nondimensionalize all the lengths by l_0, time by $\zeta l_0^2/k_BT$, energy by k_BT, and diffusivity by k_BT/ζ, where $\zeta = 3\pi\mu\sigma$ is the friction coefficient of the bead. The initial configuration is constructed with the procedures used in our previous work.[5] The system is equilibrated first by 1×10^6 off-lattice Monte Carlo (MC) steps with the standard Metropolis algorithm,[35] and then by 1×10^4 additional Brownian dynamics (BD) steps with $\Delta t = 0.0005$, taking into account HI. After the system has been equilibrated, the data is collected in the next 1×10^6 BD steps with HI effect. At least three independent runs are carried out for each case and the average is taken so as to reduce the statistical error. Because of statistical inaccuracy, some long-time dynamical results at large N_{total} are omitted in the figures shown in Section 3.

3. Results and Discussion

Brownian motion of macromolecules in a solvent can be distinguished into short- and long-time diffusion. At a small time scale in which the object diffuses a distance much smaller than its own size, the random motion is regarded as short-time diffusion that is affected purely by a hydrodynamic effect averaged over the instantaneous equilibrium configurations. In contrast, the long-time diffusivity involves a larger time, over which the object diffuses a distance larger than its size and is influenced by memory effect arising from evolution of configuration and/or interactions among the entities. In principle, a rather long simulation time is required to obtain a precise long-time diffusivity. This task, however, could become practically difficult due to the limitation of CPU power.

The short-time diffusivity can be determined by taking average for the trace of the mobility tensor and is expressed by the Kirkwood formula[36,37]

$$D^{\mathrm{K}} = \frac{k_BT}{3N_{\mathrm{total}}^2}\sum_{i,j}^{N_{\mathrm{total}}} \mathrm{Tr}\langle\mathbf{M}_{ij}\rangle \tag{10}$$

where $\langle\ \rangle$ denotes an ensemble average. Applying the Rotne−Prager−Yamakawa tensor to eq 1 yields

$$D^{\mathrm{K}} = \frac{D_0}{N_{\mathrm{total}}} + \frac{k_BT}{6\pi\mu N_{\mathrm{total}}^2}\sum_{i\neq j}\left\langle\frac{1}{r_{ij}}\right\rangle \tag{11}$$

where r_{ij} is the distance between bead i and j. D^{K} can be calculated by either MC or BD simulation because it requires only instantaneous equilibrium chain conformations. In principle, the short-time diffusivity can alternatively be determined by the mean-square displacement (MSD) of the mass center of the conjugate:

$$D_{\mathrm{S}} = \lim_{t\to 0}\frac{\mathrm{MSD}(t)}{6t} \tag{12}$$

provided that the time period used in the calculation is sufficiently small, yet with Δt much longer than the momentum relaxation time of the constituting beads. These two methods indeed produce an equal short-time diffusivity, as demonstrated in Figure 2, where we plot the diffusivity of a dendrimer and of a dendrimer−polymer conjugate as functions of the corresponding mean-square radii of gyration. The slope of the line in the log−log plot is about −0.5, clearly indicating the applicability of the Stokes−Einstein relationship. The numeric values of D^{K} and D_{S} are also listed in Tables1 and 2.

Figure 3 shows the short-time diffusivity of a dendrimer−polymer conjugate with varying length of attached chains as a function of the total number of beads. For a free-draining model, the friction coefficient of the conjugate is the sum of the friction coefficients of all the individual beads, each simply given by the Stokes law. In our simulation, all beads are of the same size and so are their friction coefficients. Therefore, the diffusivity of a free-draining conjugate is expected to be inversely proportional to the total number of beads of the conjugate. Our simulated dependence of D_{S} on $1/N_{\mathrm{total}}$ for a free-draining model is nearly linear, in agreement with the expectation. If HI is taken into account, the frictional resistance experienced by each bead is reduced because of the hydrody-

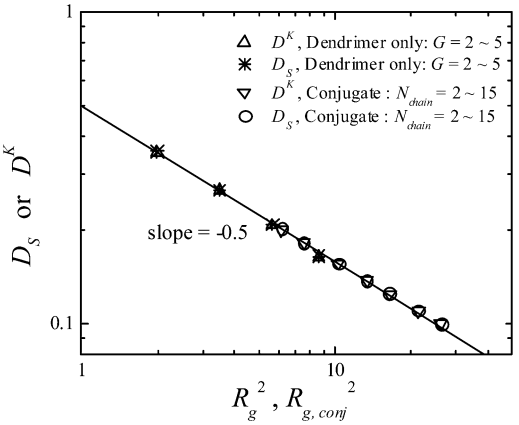

Figure 2. Short-time diffusivity as a function of radius of gyration.

Table 1. Simulation Results for Dendrimers and the Exponents of Power Laws

	R_g^2	D^{K}	D_{S}	D_{L}
$G = 2$	1.98	0.36	0.36	0.33
$G = 3$	3.50	0.27	0.27	0.25
$G = 4$	5.65	0.21	0.21	0.20
$G = 5$	8.63	0.16	0.17	0.15
ν ($\sim R_g^{-\nu}$)		1.05	1.05	1.06

Table 2. Simulation Results for Dendrimer−Polymer Conjugates and the Exponents of Power Laws

	$R_{g,conj}^2$	D^{K}	D_{S}	D_{L}
$G = 3$, $N_{chain} = 0$	3.50	0.27	0.27	0.25
$G = 3$, $N_{chain} = 2$	6.15	0.20	0.20	0.20
$G = 3$, $N_{chain} = 3$	7.51	0.18	0.18	0.16
$G = 3$, $N_{chain} = 5$	10.28	0.16	0.16	0.13
$G = 3$, $N_{chain} = 7$	13.30	0.14	0.14	0.12
ν ($\sim R_{g,conj}^{-\nu}$)		0.99	1.00	1.18

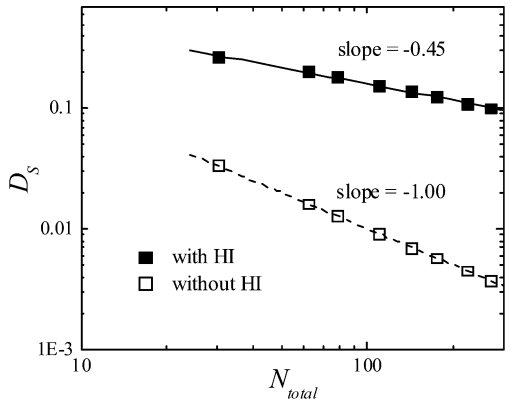

Figure 3. Short-time diffusivity as a function of total number of beads.

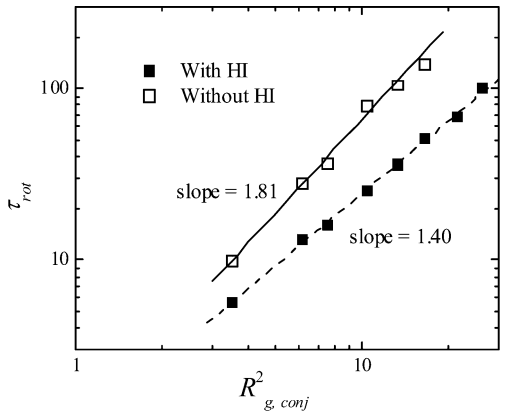

Figure 4. Rotational relaxation time of a conjugate as a function of radius of gyration.

namic screening caused by the other beads, thereby leading to an increase in diffusivity when compared with a free-draining model, as shown in Figure 3. Our simulation finds that the dependence of D_S on N_{total} up to $N_{chain} = 15$ follows a power law with the exponent equal to -0.45, which is stronger than that for a dendrimer (≈ 0.32, obtained from G2 to G7).[5] This behavior makes sense because the conjugate is composed of a dendrimer core and periphery linear chains; the two moieties are structurally different. It should be noted that the power of -0.45 is different from -0.771 reported in our prior study, where longer grafted chains ($7 \leq N_{chain} \leq 30$) are used (see Figure 16 of ref 5). In fact, that work has found that the grafted polymers become brushlike when they are long enough. As such, each of the chains, when isolated, would show a diffusional behavior, which scales as $\ln N_{chain}/N_{chain}$. It therefore implies a stronger dependence of the conjugate diffusivity on the total bead number when N_{chain} increases.

The long-time diffusion can be determined from MSD of the mass center by

$$D_L = \lim_{t\to\infty} \frac{\mathrm{MSD}(t)}{6t} \tag{13}$$

In principle, accurate D_L can be obtained by using a very large t. However, it requires an infeasibly long computation time, primarily because the time-consuming decomposition of the mobility tensor scales as $N_{total}^{2.25}$.[34] To avoid this difficulty, we adopt an approach similar to that of Lyulin et al.[25] to calculate D_L based on MSD ranging from a squared gyration radius up to 20. The results for dendrimers and conjugates are tabulated in Tables 1 and 2, respectively. The power-law exponent ($D \sim R_g^{-\nu}$) is also shown in the last row of each table. Under an athermal condition, Lyulin et al.[25] recently reported $D_L \sim R_g^{-0.8}$ for dendrimers using the simulation results for up to three generations in their defined model (N ranging from 4 to 46), while they also obtained $D_L \sim N^{-0.35}$ in the same work. A combination of the two findings leads to a scaling relationship $R_g \sim N^{0.43}$, which is consistent with the listed R_g in their Table 1. This strong N dependence of R_g is different from $R_g \sim N^{1/3}$ obtained by other researchers.[5,10,12] It is partly attributable to the inclusion of the results for small N in the determination of the scaling power. For example, their data will give $R_g \sim N^{0.37}$ if the result for $N = 4$ is excluded. Using Table 1, we find that $R_g \sim N^{0.33}$, with N ranging from 14 to 126, is in better agreement with the literature value. It can be found that both short-time and long-time diffusivities are nearly inversely proportional to R_g. Our recent MC simulation has indeed obtained $D^K \sim N^{-0.32}$ and $R_g \sim N^{0.31}$ for dendrimers from G2 to G7,[5] showing a similar behavior $D^K \sim R_g^{-1.04}$. From Tables 1 and 2, one can also see that D_L is slightly smaller than D_S for either a dendrimer or a conjugate as expected. For conjugates, our results for D_L in Table 2 show a slightly stronger dependence on R_g than expected ($\nu = 1$), because of limited accuracy associated with the insufficiently long times used.

Table 3. Comparison of $\tau_{rot} \sim N^{\nu}$ for Dendrimers

	ν		
	this study	Lyulin et al.[22]	Cai and Chen[19,20]
without HI	1.47	1.6	1.0
with HI	1.08	1.3	1.1

The rotational diffusion of a dendrimer−polymer conjugate as a whole can be characterized by the time correlation function,

$$C_{rot}(t) = \frac{1}{N_{end}} \sum_i \langle \mathbf{e}_i(0)\cdot\mathbf{e}_i(t)\rangle \tag{14}$$

with

$$\mathbf{e}_i = \frac{\mathbf{r}_{ei} - \mathbf{r}_{C,conj}}{|\mathbf{r}_{ei} - \mathbf{r}_{C,conj}|}$$

where $\mathbf{r}_{ei}$ is the position of the free end bead of the ith grafted chain, and $\mathbf{r}_{C,conj}$ is the center of mass of the conjugate. Because the correlation function in principle decays exponentially with time, we determine the relaxation time τ_{rot} from $\ln C_{rot}(\tau_{rot}) = -1$. Figure 4 plots τ_{rot} of a conjugate against its $R^2_{g,conj}$ for both the free-draining case and the case with HI. Similar to our recent results for a linear polyelectrolyte,[38] ignoring HI leads to slower rotational dynamics of the conjugate because of the absence of hydrodynamic shielding. We also carry out simulations for dendrimers (G2 to G5) without grafted chains and show the results and comparison in Table 3. Our result for the case with HI agrees well with Chen and Cai's prediction,[23] which is based on a preaveraging HI approximation. The better agreement than that obtained by Lyulin et al.[25] is probably due to the flexible spacer used in our simulation. Moreover, using the exponent shown in Table 3 and the scaling behavior of R_g from our simulations finds $\tau_{rot} \sim R_g^{3.2}$, which is similar to $\tau_{rot} \sim R^3$ of an impermeable sphere with radius R. When HI is neglected, the powers predicted from this study and Lyulin et al.[25] are quite different from that of Cai and Chen,[19] who did not consider the excluded volume effect. For dendrimer−polymer conjugates, our simulation results in Figure 4 yield $\tau_{rot} \sim R^{2.8}_{g,conj}$ with HI effects, as opposed to $\tau_{rot} \sim R^{3.62}_{g,conj}$ for the free-draining case. For the former, the slight deviation of the exponent from the

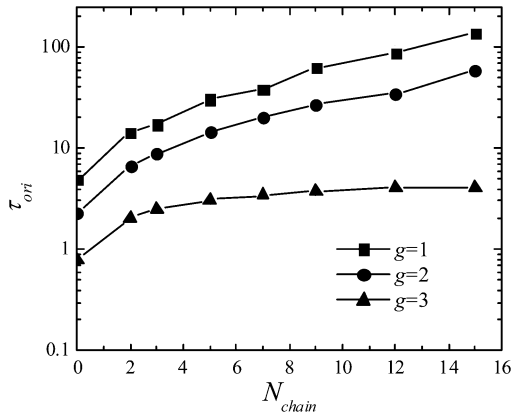

Figure 5. Reorientation relaxation time of bonds of the dendrimer core as a function of the length of grafted chains.

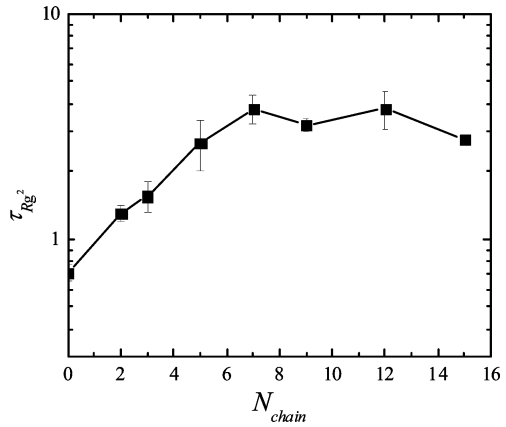

Figure 6. Relaxation time of the gyration-radius fluctuation of a conjugate as a function of the length of grafted chains.

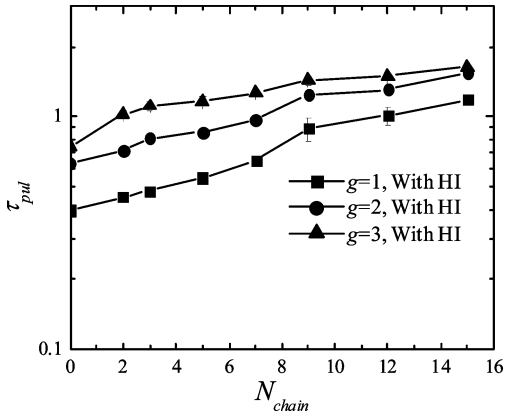

Figure 7. Relaxation time of internal pulsation for different generations as a function of the length of grafted chains.

expected value of 3 is due to insufficient accuracy in the simulations. Both the translational diffusivity and the rotational relaxation time of a conjugate depend more strongly on the total number of beads than the dendrimer counterparts. This behavior can be explained by the hybrid rotational dynamics of the dendrimer core and the grafted chains. The reorientation dynamics of the grafted chains will be analyzed in more detail later.

The local reorientation of a single bond inside the dendrimer can be explored by the correlation function

$$C_{\text{ori}}(t) = \frac{1}{N_g}\sum_i \langle \mathbf{b}_{i,g}(0)\cdot\mathbf{b}_{i,g}(t)\rangle \qquad (15)$$

where $\mathbf{b}_{i,g}$ is the unit vector between two bonded beads at the gth and $(g-1)$th generation of the dendrimer, and N_g is the bead number in the gth generation. The corresponding relaxation time τ_{ori} is plotted as a function of N_{chain} in Figure 5. As expected, slower reorientation dynamics is obtained for the bonds at lower generations of the dendrimer because the reorientation involves the motion of a bigger substructure linked to the bead. It is interesting to find that the relaxation time for the most outer bonds of the dendrimer core ($g = 3$) appears to approach a constant at large N_{chain}.

The dynamics of the size fluctuation of a dendrimer−polymer conjugate can be characterized by the correlation function

$$C_{R_g^2}(t) = \frac{\langle R^2_{\text{g,conj}}(0)R^2_{\text{g,conj}}(t)\rangle - \langle R^2_{\text{g,conj}}\rangle^2}{\langle R^4_{\text{g,conj}}\rangle - \langle R^2_{\text{g,conj}}\rangle^2} \qquad (16)$$

The relaxation of $C_{R_g^2}(t)$ is associated with the internal motion of the conjugate and is thus independent of the conjugate rotation. The corresponding relaxation time $\tau_{R_g^2}$ is plotted against the chain length in Figure 6. It can be found that $\tau_{R_g^2}$ is significantly smaller than the rotational relaxation time τ_{rot} shown in Figure 4. There exist three effects when the attached chains increase in length: (1) reduced back-folding of the terminal segments of the dendrimer core because of the increased steric effect,[5] leading to a more ordered and rigid core structure; (2) increased flexibility of the conjugate due to the grafted linear polymers; (3) increased hydrodynamic dampening as the total number of beads increases. Our simulation results show that the combination of the latter two effects appears greater than the former, and therefore, $\tau_{R_g^2}$ increases with N_{chain}, but levels off for $N_{\text{chain}} \geq 7$, for which the grafted polymers are found to become brushlike in our prior work.[5] To complement the analysis, we also examine the internal pulsation of the dendrimer core by monitoring the motions of beads belonging to the same generation through the correlation function

$$C_{\text{pul}}(t) = \frac{1}{N_g}\sum_i \frac{\langle h^2_{i,g}(0)h^2_{i,g}(t)\rangle - \langle h^2_{i,g}\rangle^2}{\langle h^4_{i,g}\rangle - \langle h^2_{i,g}\rangle^2} \qquad (17)$$

with

$$h^2_{i,g} = (\mathbf{r}_{i,g} - \mathbf{r}_{\text{C}})^2$$

where $\mathbf{r}_{i,g}$ is the position of the ith bead in the gth generation, and $\mathbf{r}_{\text{C}}$ is the center of mass of the dendrimer core. The corresponding relaxation time τ_{pul} is plotted against the length of the grafted chains for different generations in Figure 7. It is evident that the pulsation is slowed by the grafted chains, and the effect becomes stronger with increasing chain length. The relaxation is slower for the more exterior generation. From Figure 7, we can conclude that the grafted polymers slow the size fluctuation of the dendrimer core.

Our prior MC simulation[5] has found that, at sufficient length, the attached chains become brushlike owing to an increased steric effect. For an isolated rodlike chain of sufficient length, the rotational relaxation time scales as N^3_{chain} without HI and as $N^3_{\text{chain}}/(\ln N_{\text{chain}}/2)$ with HI.[39] To explore the reorientation dynamics of the grafted chains, we calculate the correlation function

$$C_{\text{chain}}(t) = \frac{1}{N_{\text{end}}}\sum_i \langle \mathbf{v}_i(0)\cdot\mathbf{v}_i(t)\rangle \qquad (18)$$

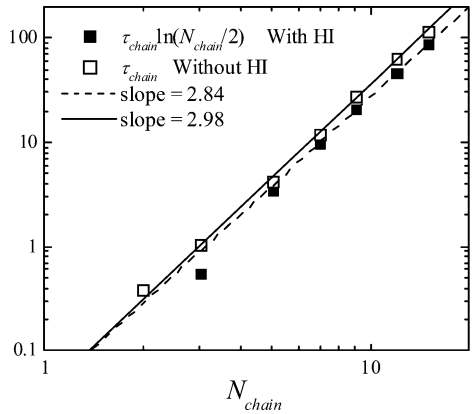

Figure 8. Dependence of reorientation relaxation time of grafted chains on their length.

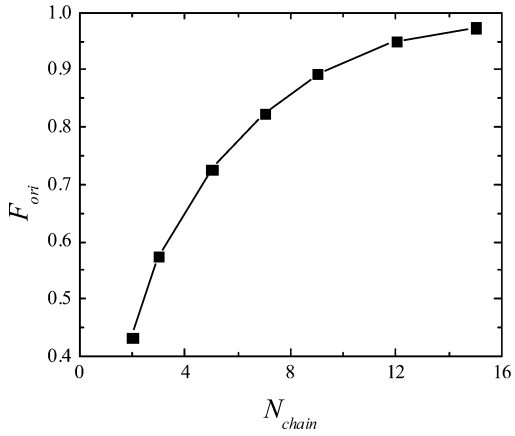

Figure 9. Average projection of chain orientation in the radial direction as a function of the length of grafted chains.

with

$$\mathbf{v}_i = \mathbf{R}_{i,\mathrm{ete}}/R_{i,\mathrm{ete}}$$

where $\mathbf{R}_{i,\mathrm{ete}}$ is the end-to-end vector of the ith grafted chain. The corresponding relaxation time τ_{chain} can then be determined. In Figure 8, we plot τ_{chain} and $\tau_{\mathrm{chain}}\ln(N_{\mathrm{chain}}/2)$ against the chain length for the cases without and with HI, respectively. The linear fitting for $N_{\mathrm{chain}} \geq 7$ in the log−log plot finds $\tau_{\mathrm{chain}} \sim N_{\mathrm{chain}}^{2.98}$ for the free-draining cases and $\tau_{\mathrm{chain}}\ln(N_{\mathrm{chain}}/2) \sim N_{\mathrm{chain}}^{2.84}$ for the cases with HI. The behavior is very similar to that of an isolated rodlike chain, although the HI and steric effects from neighboring chains do exist. For the cases with HI, the slight deviation of the power from 3 can be attributed in part to the investigated values of N_{chain} that are not very large. To better understand the reorientation of the grafted chains, we examine their average orientation by calculating

$$F_{\mathrm{ori}} = \frac{1}{N_{\mathrm{end}}}\sum_i \left\langle \mathbf{v}_i \cdot \frac{\mathbf{R}_{i,\mathrm{etc}}}{R_{i,\mathrm{etc}}} \right\rangle \qquad (19)$$

where $\mathbf{R}_{i,\mathrm{etc}}$ is the vector from the mass center of the conjugate to the free end of the ith grafted chain. The results are shown as a function of the chain length in Figure 9. It can be found that the grafted chains are oriented radially on average when they are long enough. This provides additional evidence to support the conclusion obtained from the static results in our prior work[5] that long attached chains are brushlike. To check if the effect of neighboring chains is weak, we estimate the average volume occupied by each of the grafted chain. For the longest chain length $N_{\mathrm{chain}} = 15$ examined in this study, the radius of dendrimer core is about 2.6 and the end-to-end distance of the grafted chain is 7.1.[5] Accordingly, the volume of the spherical shell housing the grafted chains can be estimated, and then be divided by N_{end}, to give the average volume per chain. The cubic root of this average volume is found to be 6.2, which is comparable to 7.1. For brushlike chains, this condition is around the limit of the dilute regime, so the interchain interactions are not strong.[39] As such, each of the grafted chains can be regarded as reorienting within a conical region on average, and the chain-length dependence of the reorientation is not much affected by the neighboring chains.

When the grafted chains become very long, a conjugate is expected to behave as a star polymer, where the dendrimer is equivalent to the star core. The grafted chains are thus no longer brushlike. This limiting case is beyond the scope of the present study with $N_{\mathrm{chain}} \leq 15$. Verification of this asymptotic behavior for dynamics would be computationally difficult because of a very large N_{total} incurred.

4. Conclusion

We have conducted BD simulation to investigate the dynamics of dendrimers and dendrimer−polymer conjugates based on a coarse-grained bead−spring model. The grafted polymers are found to slow the global dynamics of the dendrimer core. Despite the structural difference between the two moieties, the translational and rotational diffusivities in principle scale as $R_{\mathrm{g,conj}}^{-1}$ and $R_{\mathrm{g,conj}}^{-3}$, in a Stokes−Einstein fashion, analogous to polymers of other types. The local dynamics, such as the size fluctuation and the bond reorientation relaxation of the dendrimer core, is also retarded by the attached polymers. When the grafted chains are long enough, they become brushlike, evidenced by the scaling behavior of the end-to-end distance in the prior work[5] and by the chain-length dependence of the reorientation relaxation time obtained in the present study. For the range of chain length investigated, it is found that the brushlike grafted polymers do not interact strongly to render a noticeable change in the chain-length dependence of their reorientation, as compared to an isolated rodlike polymer.

Acknowledgment. We are grateful to the National University of Singapore for supporting the work through grant R-279-000-172-112.

References and Notes

(1) Aulenta, F.; Hayes, W.; Rannard, S. *Eur. Polym. J.* **2003**, *39*, 1741.
(2) Boas, U.; Heegaard, P. M. H. *Chem. Soc. Rev.* **2004**, *33*, 43.
(3) Liu, M.; Kono, K.; Fréchet, J. M. J. *J. Polym. Sci., Part A: Polym. Chem. Ed.* **1999**, *37*, 3492.
(4) Kojima, C.; Kono, K.; Maruyama, K.; Takagishi, T. *Bioconjugate Chem.* **2000**, *11*, 910.
(5) Zhou, T.; Chen, S. B. *Macromolecules* **2005**, *38*, 8554.
(6) Sheng, Y.-J.; Jiang, S.; Tsao, H. K. *Macromolecules* **2002**, *35*, 7865.
(7) Giupponi, G.; Buzza, D. M. A. *J. Chem. Phys.* **2004**, *120*, 10290.
(8) Lescanec, R. L.; Muthukumar, M. *Macromolecules* **1990**, *23*, 2280.
(9) Mansfield, M. L.; Klushin, L. I. *Macromolecules* **1993**, *26*, 4262.
(10) Murat, M.; Grest, S. *Macromolecules* **1996**, *29*, 1278.
(11) Mansfield, M. L. *Macromolecules* **2000**, *33*, 8043.
(12) Maiti, P. K.; Cağin, T.; Wang, G.; Goddard, W. A. *Macromolecules* **2004**, *37*, 6236.
(13) Meltzer, A. D.; Tirrell, D. A.; Jones, A. A.; Inglefield, P. T.; Hedstrand, D. M.; Tomalia, D. A. *Macromolecules* **1992**, *25*, 4541.
(14) Meltzer, A. D.; Tirrell, D. A.; Jones, A. A.; Inglefield, P. T. *Macromolecules* **1992**, *25*, 4549.
(15) Mourey, T. H.; Turner, S. R.; Rubinstein, M.; Fréchet, J. M. J.; Hawker, C. J.; Wooley, K. L. *Macromolecules* **1992**, *25*, 2401.
(16) Scherrenberg, R.; Coussens, B.; van Vliet, P.; Edouard, G.; Brackman, J.; de Brabander, E. *Macromolecules* **1998**, *31*, 456.
(17) Rietveld, I. B.; Bedeaux, D.; *Macromolecules* **2000**, *33*, 7912.

(18) Mansfield, M. L.; Klushin, L. I. *J. Phys. Chem.* **1992**, *96*, 3994.
(19) Ganazzoli, F.; la Ferla, R.; Terragni, G. *Macromolecules* **2000**, *33*, 6611.
(20) la Ferla, R. *J. Chem. Phys.* **1997**, *106*, 688.
(21) Ganazzoli, F.; la Ferla, R.; Raffaini, G. *Macromolecules* **2001**, *34*, 4222.
(22) Cai, C.; Chen, Z. Y. *Macromolecules* **1997**, *30*, 5104.
(23) Chen, Z. Y.; Cai, C. *Macromolecules* **1999**, *32*, 5423.
(24) Karatasos, K.; Adolf, D. B.; Davies, G. R. *J. Chem. Phys.* **2001**, *115*, 5310.
(25) Lyulin, S. V.; Darinskii, A. A.; Lyulin, A. V.; Michels, M. A. J. *Macromolecules* **2004**, *37*, 4676.
(26) Stark, B.; Stühn, B.; Frey, H.; Lach, C.; Lorenz, K.; Frick, B. *Macromolecules* **1998**, *31*, 5415.
(27) Rey, A.; Freire, J. J.; de la Torre, J. G. *Macromolecules* **1987**, *20*, 2385.
(28) Öttinger, H. C. *The Stochastic Processes in Polymeric Fluids*; Springer-Verlag: Berlin, 1996.
(29) Yamakawa, H. *J. Chem. Phys.* **1970**, *53*, 436.
(30) Ronte, J.; Prager, S. *J. Chem. Phys.* **1969**, *50*, 436.
(31) Ermak, D. L.; McCammon, J. A. *J. Chem. Phys.* **1978**, *69*, 1352.
(32) Canuto, C.; Hussaini, M. Y.; Quarteroni, A.; Zang, T. A. *Spectral Methods in Fluid Dynamics*; Springer-Verlag: New York, 1987.
(33) Fixman, M. *J. Chem. Phys.* **1983**, *78*, 1588.
(34) Jendrejack, R. M.; Graham, M. D.; de Pablo, J. J. *J. Chem. Phys.* **2000**, *113*, 2894.
(35) Allen, M. P.; Tildesley, D. J. *Computer Simulation of Liquids*; Oxford University Press: Oxford, 1987.
(36) Kirkwood, J. G. *J. Polym. Sci.* **1954**, *12*, 1.
(37) Liu, B.; Dunweg, B. *J. Chem. Phys.* **2003**, *118*, 8061.
(38) Zhou, T.; Chen, S. B. *J. Chem. Phys.* **2006**, *124*, 034904.
(39) Doi, M.; Edwards, S. F. *The Theory of Polymer Dynamics*; Oxford University Press: Oxford, 1986.

MA061103Q